JOURNAL OF VIROLOGY, July 2010, p. 6900–6908 Vol. 84, No. 14
0022-538X/10/$12.00 doi:10.1128/JVI.01742-09

Interferon Regulatory Factor 3 Attenuates Reovirus Myocarditis and Contributes to Viral Clearance▽

Geoffrey H. Holm,[1] Andrea J. Pruijssers,[2,4] Lianna Li,[5] Pranav Danthi,[2,4]† Barbara Sherry,[5,6] and Terence S. Dermody[2,3,4]*

Department of Biology, Colgate University, Hamilton, New York 13346[1]; Departments of Pediatrics[2] and Microbiology and Immunology,[3] and Elizabeth B. Lamb Center for Pediatric Research,[4] Vanderbilt University School of Medicine, Nashville, Tennessee 37232; and Departments of Molecular Biomedical Sciences[5] and Microbiology,[6] North Carolina State University, Raleigh, North Carolina 27606

Received 18 August 2009/Accepted 30 April 2010

Apoptosis is a pathological hallmark of encephalitis and myocarditis caused by reovirus in newborn mice. In cell culture models, the antiviral transcription factor interferon regulatory factor 3 (IRF-3) enhances reovirus-induced apoptosis following activation via retinoic acid inducible gene I and interferon promoter-stimulating factor 1. To determine the role of IRF-3 in reovirus disease, we infected newborn IRF-3$^{+/+}$ and IRF-3$^{-/-}$ mice perorally with mildly virulent strain type 1 Lang (T1L) and fully virulent strain type 3 SA+ (T3SA+) and monitored infected animals for survival. Both wild-type and IRF-3$^{-/-}$ mice succumbed with equivalent frequencies to infection with T3SA+. However, the absence of IRF-3 was associated with significantly decreased survival rates following infection with T1L. The two virus strains achieved similar peak titers in IRF-3$^{+/+}$ and IRF-3$^{-/-}$ mice in the intestine, brain, heart, liver, and spleen. However, by day 12 postinoculation, titers in all organs examined were 10- to 100-fold higher in IRF-3$^{-/-}$ mice than those in wild-type mice. Increased titers were associated with marked pathological changes in all organs examined, especially in the heart, where absence of IRF-3 resulted in severe myocarditis. Cellular and humoral immune responses were equivalent in wild-type and IRF-3$^{-/-}$ animals, suggesting that IRF-3 functions independently of the adaptive immune response to enhance reovirus clearance. Thus, IRF-3 serves to facilitate virus clearance and prevent tissue injury in response to reovirus infection.

Pathological consequences of viral infection are determined by interactions between viral virulence factors and host antiviral responses. Viral replication and immune evasion strategies facilitate viral dissemination and transmission but are countered by both innate and adaptive immune responses that limit virus growth and facilitate virus clearance. The interplay between these processes determines whether viral infection is asymptomatic or progresses to produce disease. While virus-host interactions are becoming increasingly well defined using cell culture models, mechanisms that contribute to viral pathogenesis at the organismal level are less well understood.

Mammalian orthoreoviruses (reoviruses) have been used as models for studies of viral pathogenesis. Reoviruses are enteric, nonenveloped viruses with a double-stranded RNA (dsRNA) genome (29). Peroral (p.o.) inoculation of newborn mice with reovirus leads to a disseminated infection that causes damage to the central nervous system (CNS), heart, and liver (40). Strain-specific differences in reovirus tropism and virulence are linked to both viral and host factors. Viral factors include receptor utilization (1, 3, 42) and sensitivity to type 1 interferons (IFNs) (32), while host factors include components of innate and adaptive immunity (38, 39). Protection against reovirus infection is mediated by both cell-mediated and humoral immune mechanisms. Depletion of either CD4$^+$ or CD8$^+$ T cells abrogates or severely inhibits cell-mediated immune protection against reovirus infection (30), whereas exogenously administered anti-reovirus antibodies limit reovirus spread to the CNS (36). These adaptive immune mechanisms are for the most part serotype independent and display differences in efficacy depending on the tropism of the infecting strain (39).

Innate immune responses also can limit systemic spread of reovirus and modulate reovirus-induced tissue injury. Type 1 IFNs produced by Peyer's patch conventional dendritic cells control intestinal reovirus infection and prevent systemic spread (15). Additionally, the innate immune transcription factor nuclear factor-κB (NF-κB) mediates organ-specific differences in reovirus cell injury and disease (24). NF-κB is required for reovirus-induced apoptosis in the CNS and contributes to the development of encephalitis (8, 24), whereas it functions in prosurvival mechanisms in the heart via the induction of type 1 IFNs (24). These observations suggest that in addition to, or in conjunction with, adaptive immune pathways, innate immune pathways influence reovirus pathogenesis. However, the coordinated action of these processes is complex and not well defined.

Several reports have characterized cellular sensors and molecular pathways that activate the innate immune response induced by reovirus infection. Despite the dsRNA nature of the reovirus genome, Toll-like receptor 3 (TLR3) is not required for limiting reovirus infection in mice (9, 15). Instead, the cytoplasmic RNA sensor, retinoic acid inducible gene I

* Corresponding author. Mailing address: Lamb Center for Pediatric Research, D7235 MCN, Vanderbilt University School of Medicine, Nashville, TN 37232. Phone: (615) 343-9943. Fax: (615) 343-9723. E-mail: terry.dermody@vanderbilt.edu.

† Present address: Department of Biology, Indiana University Bloomington, Bloomington, IN 47405.

▽ Published ahead of print on 12 May 2010.

(RIG-I), and the RIG-I adaptor, interferon promoter-stimulating factor 1 (IPS-1), are required for activation of innate immune response transcription factors, including interferon regulatory factor 3 (IRF-3) and NF-κB, which direct the induction of a broad network of antiviral genes (5, 13, 19, 25). A major component of this response is the secretion of the antiviral cytokine, beta IFN (IFN-β). Mechanisms of IFN induction and function following reovirus infection are cell type specific (23, 43). In newborn mice, IFN-β protects against reovirus-mediated myocardial injury (24, 32). Concordantly, the capacity of reovirus strains to induce IFN-β, along with their sensitivity to this cytokine, is inversely correlated with myocarditis severity (32), suggesting that IFN-dependent processes are key determinants of reovirus pathogenesis.

In addition to the induction of type 1 IFNs, both IRF-3 and NF-κB are required for reovirus-induced apoptosis in cell culture (5, 13). Ablation of the p50 and p65 (RelA) subunits of NF-κB renders fibroblast cells resistant to reovirus-induced apoptosis (5). Proapoptotic activation of p50 and p65 requires signaling via inhibitor of κB kinase α (IKKα) and NF-κB essential modulator (NEMO) but not NF-κB-inducing kinase (NIK) (12). This proapoptotic role for NF-κB in reovirus infection also has been observed in the murine CNS but not in the heart (24). Additionally, IRF-3 is required for enhanced apoptosis in response to reovirus infection in cultured cells (13). However, the function of IRF-3 in reovirus infection of newborn mice is not known.

Several RNA viruses induce the expression of type 1 IFNs via the activation of both IRF-3 and the related transcription factor IRF-7 (21, 27, 28). IRF-3-deficient mice are more susceptible to lethal infection by some neurotropic RNA viruses, such as encephalomyocarditis virus (27) and West Nile virus (7). However, induction of type 1 IFNs following infection with these viruses does not substantially differ in IRF-3-deficient mice in comparison to that in wild-type controls (7, 14). These reports indicate that IRF-3 regulates cell-specific responses that protect against RNA virus infection by both induction of type 1 IFNs and IFN-independent mechanisms, such as altering the basal expression of innate immune response genes, including RIG-I, melanoma differentiation associated gene-5 (Mda-5), and antiviral interferon-stimulated genes (ISGs) (7).

In this study, we examined the functional consequences of IRF-3 deficiency in reovirus pathogenesis. We found that IRF-3 influences survival following reovirus infection in a serotype-dependent manner. Mice lacking IRF-3 displayed a diminished type I IFN response at the primary site of infection at early times postinoculation. Peak viral titers at sites of secondary replication were equivalent in wild-type and IRF-3-deficient animals. However, viral titers and virus-induced pathology at these sites were more substantial in the absence of IRF-3 at late times postinoculation, suggesting that IRF-3-dependent responses are required for efficient reovirus clearance. Differences in viral titer and tissue damage did not correlate with ineffective priming of the adaptive immune response, as $CD8^+$ T-cell IFN-γ responses and serum IgG levels were equivalent in infected wild-type and IRF-3-deficient mice. Together, these results suggest a novel, cell-intrinsic role for IRF-3 in IFN-independent innate immune processes that influence viral clearance.

MATERIALS AND METHODS

Cells and viruses. Murine L929 cells were maintained in Joklik's minimal essential medium supplemented to contain 10% fetal bovine serum (FBS), 2 mM L-glutamine, 100 U/ml penicillin, 100 μg/ml streptomycin, and 25 ng/ml amphotericin B (Sigma-Aldrich). Murine C57SV fibroblasts were maintained in RPMI 1640 medium (Sigma-Aldrich) supplemented to contain 10% FBS, 2 mM L-glutamine, 100 U/ml penicillin, 100 μg/ml streptomycin, and 25 ng/ml amphotericin B. Reovirus strain type 1 Lang (T1L) is a laboratory stock. Strain type 3 SA+ (T3SA+) was generated by reassortment of reovirus strains T1L and type 3 clone 44-MA (3).

Purified reovirus virions were generated from second- or third-passage L-cell lysate stocks of twice-plaque-purified reovirus as described previously (36). Viral particles were Freon extracted from infected cell lysates, layered onto 1.2- to 1.4-g/cm^3 CsCl gradients, and centrifuged at 62,000 × *g* for 18 h. Bands corresponding to virions (1.36 g/cm^3) were collected and dialyzed in virion storage buffer (150 mM NaCl, 15 mM $MgCl_2$, 10 mM Tris-HCl [pH 7.4]).

Mice. Control IRF-$3^{+/+}$ mice (C57BL/6-J) and IRF-$3^{-/-}$ mice (IRF-3 KO B6) (27) were obtained from Jackson Laboratory and Karen Mossman (McMaster University, Hamilton, Ontario, Canada), respectively. Two-day-old mice were inoculated either intracranially (i.c.) or p.o. with purified reovirus diluted in phosphate-buffered saline (PBS). Intracranial inoculations were delivered to the left cerebral hemisphere in a volume of 5 μl, using a Hamilton syringe (BD Biosciences) and a 30-gauge needle (33). Peroral inoculations were delivered in a volume of 50 μl by passage of a polyethylene catheter 0.61 mm in diameter (BD) through the esophagus and into the stomach (26). The inoculum contained 0.3% (vol/vol) green food coloring to allow the accuracy of delivery to be judged. For analysis of viral virulence, mice were monitored for weight loss and symptoms of disease for 21 days. For survival experiments, mice were euthanized when found to be moribund (defined by rapid or shallow breathing, lethargy, or paralysis). For determination of viral titer and immunohistochemical staining, mice were euthanized at various intervals following inoculation, and organs were resected. For analysis of virus growth, organs were collected in 1 ml of PBS and homogenized by freezing, thawing, and sonication. Viral titers in organ homogenates were determined by plaque assay using L929 cells (36). For immunohistochemical staining, organs were fixed overnight in 10% formalin, followed by incubation in 70% ethanol. Fixed organs were embedded in paraffin, and 5-μm histological sections were prepared. Consecutively obtained sections were stained with hematoxylin and eosin (H&E) for evaluation of histopathologic changes or processed for immunohistochemical detection of reovirus antigens or activated caspase-3 (24). For extraction of RNA, organs were homogenized in Trizol reagent (Invitrogen) and processed according to the manufacturer's protocol. Animal husbandry and experimental procedures were performed in accordance with Public Health Service policy and the recommendations of the Association for Assessment and Accreditation of Laboratory Animal Care and approved by the Vanderbilt University School of Medicine Institutional Animal Care and Use Committee and by the North Carolina State University Institutional Animal Care and Use Committee.

Generation and infection of primary cardiac myocyte cultures. Primary cardiac myocyte cultures were generated from term fetuses or 1-day-old neonates by successive trypsinization of the apical two-thirds of the heart and selective plating as described previously (43). Cardiac myocytes (10^6) were plated onto 24-well plates (Costar) and incubated for 2 days. Overlying medium was removed, duplicate wells of cells were incubated with either medium or CsCl-purified reovirus at a multiplicity of infection (MOI) of 10 PFU/cell for 1 h, additional medium was added, and cells were incubated for 8 or 24 h. Immunofluorescence microscopy of similar cultures by the use of anti-myomesin and anti-vimentin antibodies revealed <5% fibroblast contamination of the myocyte cultures (43).

RNA isolation and quantitative reverse transcription-PCR (qRT-PCR). Primary cardiac myocyte cultures were infected with reovirus and incubated for various intervals. Medium overlying the myocytes cultures was removed, total RNA was harvested using RNeasy (Qiagen), and contaminating genomic DNA was eliminated using RNase-free DNase I (Qiagen). cDNA was generated using oligo(dT) and AMV reverse transcriptase (Promega) and amplified using primers specific for GAPDH (glyceraldehyde-3-phosphate dehydrogenase) (forward, GGG TGT GAA CCA CGA GAA AT; reverse, CCT TCC ACA ATG CCA AAG TT), IFN-β (forward, GGA GAT GAC GGA GAA GAT GC; reverse, CCC AGT GCT GGA GAA ATT GT), and ISG56 (forward, TGG CCG TTT CCT ACA GTT TC; reverse, TCC TCC AAG CAA AGG ACT TC) in Quantitech master mix (Qiagen) by using an iCycler iQ fluorescence thermocycler (Bio-Rad Laboratories) as described previously (43). Quantification and melt curve analyses were performed according to the manufacturer's protocol. For each sample, the C_T (threshold cycle) for the gene of interest was normalized to

that for GAPDH. Fold induction was calculated by comparing normalized C_T values for duplicate infected samples to those of uninfected samples at the same time point.

Splenocyte isolation. Newborn mice were inoculated p.o. with either PBS (mock) or 10^7 PFU of reovirus T1L and euthanized 8 days postinoculation. Spleens were resected into 0.5 ml of murine red blood cell lysis buffer (16.96 mM Tris [pH 7.65] in 69.92 mM ammonium chloride) and individually placed into single wells of a 24-well plate on ice. Spleens were macerated for 1 min using the plunger end of a sterile 1-ml syringe, and the contents were transferred to a 15-ml conical tube on ice. The total volume was adjusted to 15 ml, and splenocytes were incubated on ice for 5 min to allow debris to settle. Debris was removed using a sterile transfer pipette, and cells were washed once with RPMI 1640 medium.

Intracellular cytokine staining. One day prior to assay, 5×10^6 C57SV fibroblasts were either mock infected or infected with reovirus T1L at an MOI of 500 PFU/cell and incubated at 37°C overnight. Cells were removed from culture dishes by trypsin treatment and washed once with RPMI 1640 medium. Freshly isolated splenocytes (10^5) and fibroblasts (10^5) were coincubated in a volume of 0.2 ml in the wells of 96-well plates (Costar) in RPMI 1640 medium supplemented with 1 μl/ml of GolgiPlug (BD Biosciences) and 10 ng/ml recombinant human interleukin-2 (hIL-2; BD Biosciences) and incubated at 37°C for 5 h. Splenocytes were removed to the wells of fresh 96-well plates and washed once with flow cytometry buffer (FACS buffer; PBS containing 5% FBS, 0.1% sodium azide, and 0.02% EDTA). Cells were incubated with a 1:100 dilution of anti-CD8-phycoerythrin (PE) (BD Biosciences) at 4°C for 30 min and washed twice with FACS buffer. Cells were incubated with 0.1 ml of Fix/Perm solution (BD Biosciences) at 4°C for 30 min, washed twice with 1× Perm/Wash buffer (BD Biosciences), and incubated with a 1:200 dilution of anti-IFN-γ–fluorescein isothiocyanate (FITC) in Perm/Wash buffer at 4°C for 30 min. Cells were washed twice with Perm/Wash and incubated in FACS buffer prior to flow cytometric analysis by using a BD LSRII flow cytometer (BD Biosciences).

Whole-virus ELISA. Whole-blood samples from euthanized mice were collected into sterile Eppendorf tubes and incubated at 4°C overnight to allow the blood to clot. Clotted blood was centrifuged at 10,000 × *g* for 5 min, and the serum was transferred to fresh tubes and stored at −80°C. Either CsCl-purified reovirus T1L (10^{10} particles) or an equivalent volume of mock-infected CsCl-purified lysate was adsorbed to the wells of a 96-well enzyme immunoassay (EIA)/radioimmunoassay (RIA) plate (Costar) in 50 μl of 50 mM carbonate-bicarbonate buffer (pH 9.6) and incubated at 4°C overnight. Wells were washed once with enzyme-linked immunosorbent assay (ELISA) wash buffer (PBS containing 0.05% Tween 20) and incubated in 0.2 ml of ELISA blocking buffer (PBS containing 0.05% Tween 20 and 5% nonfat milk) at room temperature for 3 h. The plates were washed twice with wash buffer and incubated with 4-fold serial dilutions of serum in blocking buffer at 4°C overnight. The plates were washed three times with wash buffer and incubated with a 1:1,000 dilution of secondary antibody (horseradish peroxidase [HRP]-conjugated anti-mouse IgG [GE Healthcare]) in 0.1 ml of ELISA blocking buffer at room temperature for 1 h. Wells were washed four times with wash buffer and incubated with 0.1 ml of TMB substrate (One-Step Ultra TMB-ELISA [Pierce]) for 15 min. The reaction was stopped by adding 50 μl of 2 M sulfuric acid to each well, and the A_{450} was determined by using a SpectraMax PLUS384 spectrophotometer (Molecular Devices).

RESULTS

IRF-3 is required for the induction of type I IFNs following reovirus infection of primary murine fibroblasts (13) and cardiac myocytes (23) and efficient induction of apoptosis in reovirus-infected cells (13). To determine the role of IRF-3 in reovirus pathogenesis, we first examined whether IRF-3 influences the survival of newborn mice following inoculation with reovirus strains T1L and T3SA+. T1L and T3SA+ differ in pathogenicity following infection of newborn mice. T1L is a prototype strain that displays modest virulence, causing hydrocephalus and mild myocarditis (16, 31, 39). T3SA+ is a reassortant virus containing nine gene segments from T1L and the σ1-encoding S1 gene from strain T3C44-MA. T3SA+ is highly virulent, causing lethal encephalitis and biliary injury (3, 24). We inoculated 2-day-old IRF-$3^{+/+}$ and IRF-$3^{-/-}$ C57BL/6-J mice p.o. with either 10^7 PFU of T1L or 10^4 PFU of T3SA+ (Fig. 1). Mice were monitored for signs of disease daily for 21 days and euthanized when moribund. Following inoculation with the mildly virulent strain T1L, approximately 45% of the IRF-$3^{-/-}$ animals succumbed to infection, whereas no IRF-$3^{+/+}$ mice developed detectable clinical signs (Fig. 1A) ($P < 0.001$). In contrast, the majority of IRF-$3^{+/+}$ and IRF-$3^{-/-}$ mice succumbed to infection with the highly virulent strain T3SA+ (Fig. 1B). These results suggest that IRF-3 attenuates the virulence of a moderately pathogenic but not a highly pathogenic reovirus strain.

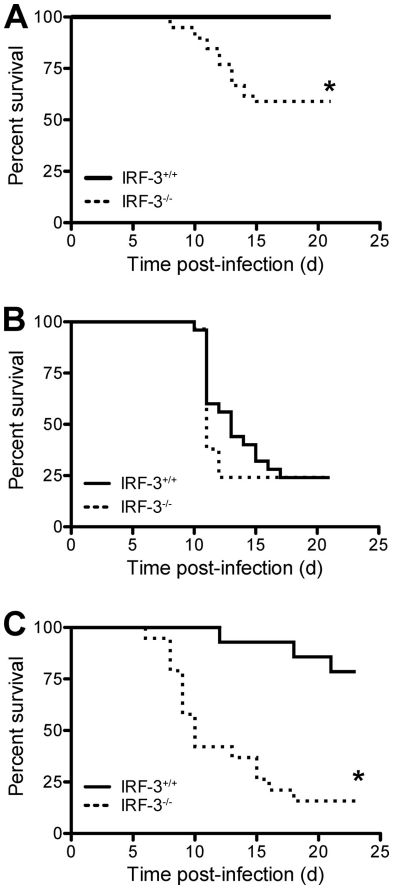

FIG. 1. IRF-3 attenuates reovirus virulence. Two-day-old IRF-$3^{+/+}$ and IRF-$3^{-/-}$ mice were inoculated with 10^7 PFU of T1L p.o. (A), 10^4 PFU of T3SA+ p.o. (B), or 10^4 PFU of T1L i.c. (C). Mice ($n = 25$ to 39) were monitored for survival for 21 days. *, $P < 0.001$ as determined by log-rank test in comparison to IRF-$3^{+/+}$ mice; d, days.

To determine whether IRF-3 influences reovirus virulence following direct inoculation into a site of secondary replication, we monitored survival after i.c. inoculation of 2-day-old IRF-$3^{+/+}$ and IRF-$3^{-/-}$ mice with 10^4 PFU of T1L. Following this route of inoculation, T1L caused lethal disease in ~20% of wild-type mice, whereas >80% of IRF-3-deficient mice succumbed to infection (Fig. 1C) ($P < 0.001$). Thus, IRF-3 attenuates reovirus virulence independent of the site of inoculation.

To test whether differences in survival following p.o. inoculation of T1L are attributable to differences in the capacity of this strain to disseminate from the initial site of replication, we quantified viral titers at sites of primary and secondary replication at various times after inoculation (Fig. 2). Reovirus T1L

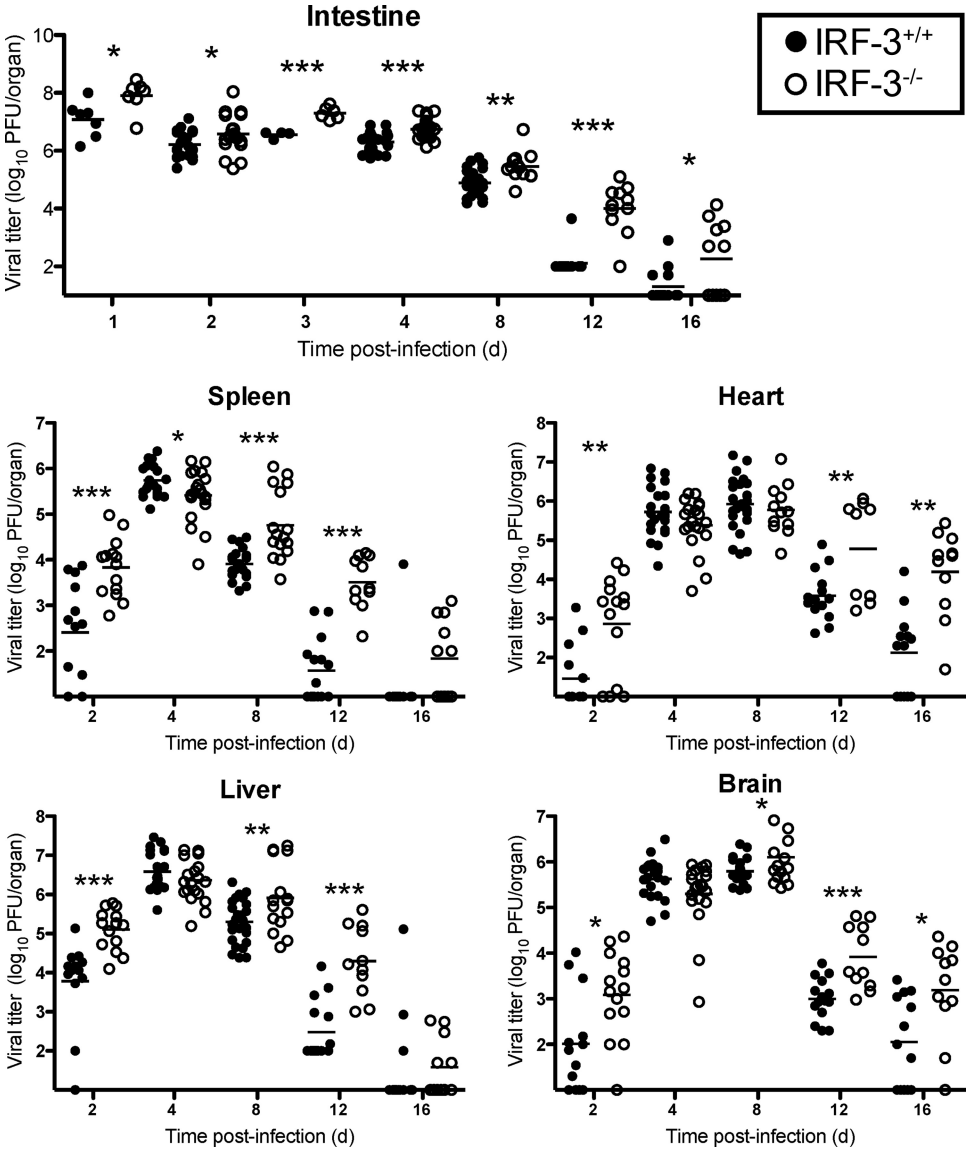

FIG. 2. IRF-3 facilitates reovirus clearance. Two-day-old IRF-$3^{+/+}$ and IRF-$3^{-/-}$ mice were inoculated p.o. with 10^7 PFU of T1L. Mice were euthanized at the times shown, and the indicated organs were resected and homogenized by freeze-thawing and sonication. Viral titers in organ homogenates were determined by plaque assay. Results are expressed as viral titer in organs of single infected animals as indicated by closed (IRF-$3^{+/+}$) or open (IRF-$3^{-/-}$) circles. Horizontal black lines indicate mean viral titers. *, $P < 0.05$; **, $P < 0.01$; and ***, $P < 0.001$, by Student's *t* test in comparison to IRF-$3^{+/+}$ mice at the same time postinoculation.

produced significantly higher titers in IRF-3-deficient animals at the site of primary replication in the intestine than it did in wild-type animals at all time points measured. Virus titers at sites of secondary replication were 10- to 100-fold higher in IRF-3-deficient animals at day 2 postinoculation, yet peak titers did not differ significantly. However, titers remained 10- to 1,000-fold higher in IRF-3-deficient animals than in wild-type animals on days 12 and 16 postinoculation, suggesting that IRF-$3^{-/-}$ mice manifest a defect in viral clearance.

Similar differences in viral titers were observed following infection of T1L by the i.c. route (data not shown). Peak titers after i.c. inoculation were slightly higher in the CNS, heart, and liver of IRF-$3^{-/-}$ mice than in those of wild-type animals. Additionally, IRF-$3^{-/-}$ mice had high virus titers in these organs at late times postinoculation when virus was not detected in wild-type mice. Together, these results suggest that IRF-3 dampens viral growth at sites of primary and secondary replication during acute infection and contributes to virus clearance independent of the inoculation route.

IFN-β is a potent antiviral cytokine that is produced in response to reovirus infection of cultured cells and *in vivo* (32). IFN-β protects neighboring cells from becoming infected by inducing an antiviral state and primes adaptive antiviral immune responses to facilitate viral clearance (6, 15, 18, 20). IRF-3 regulates the production of IFN-β in response to reovirus infection in mouse fibroblasts (13). We hypothesized that differences in viral titer observed at early times at the site of primary replication in mice might be attributable to altered

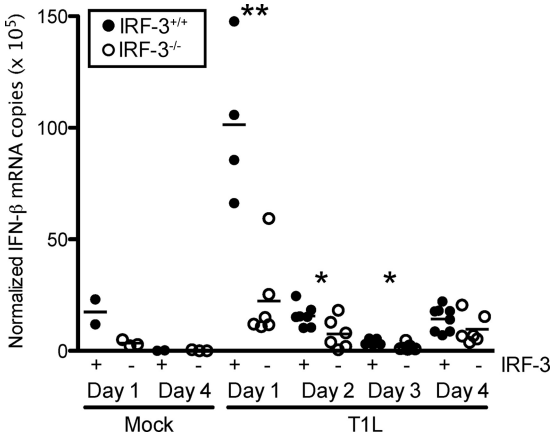

FIG. 3. IRF-3 is required for efficient IFN-β induction in the intestine at early times postinoculation. Two-day-old IRF-$3^{+/+}$ and IRF-$3^{-/-}$ mice were inoculated p.o. with 10^7 PFU of T1L. Mice were euthanized at the times shown, and the intestines were resected and homogenized. RNA was extracted from homogenized intestines, and IFN-β mRNA levels were determined by qRT-PCR relative to GAPDH. Results are expressed as normalized IFN-β mRNA copies ($\times 10^5$) in intestines of single infected animals as indicated by closed (IRF-$3^{+/+}$) or open (IRF-$3^{-/-}$) circles. Horizontal black lines indicate the mean number of normalized IFN-β mRNA copies. *, $P < 0.05$; **, $P < 0.01$ by Student's t test in comparison to IRF-$3^{+/+}$ mice at the same time postinoculation.

IFN-β production. To test this hypothesis, we quantified IFN-β mRNA levels in the intestine on days 1 through 4 postinoculation by using qRT-PCR (Fig. 3). On day 1 postinoculation, IFN-β expression levels were significantly elevated in response to T1L infection in wild-type mice, whereas expression levels in IRF-3-deficient mice were similar to those in mock-infected controls. On days 2 and 3 postinoculation, IFN-β transcript abundance decreased to levels just above background, although levels in wild-type mice were significantly greater than those in IRF-3-null mice. By day 4, significant differences in transcript abundance in the two mouse strains were not observed. These results suggest that IRF-3 influences the initial induction of IFN-β in the intestine in response to reovirus infection, which might explain the higher reovirus titers detected at that site in IRF-3-deficient mice at early times postinoculation.

IFN-β is an essential component of host defense against reovirus-induced myocarditis. Nonmyocarditic reovirus strains induce myocarditis in mice depleted of IFN-α/β (32), and reconstitution of IFN-β into mice lacking the p50 subunit of NF-κB diminishes viral titer and reduces myocardial lesions caused by reovirus (24). Dominant negative mutants of IRF-3 inhibit IFN-β induction in primary cardiac myocyte cultures (23), indicating that IRF-3 is an important inducer of the type 1 IFN response in heart tissue. Therefore, we reasoned that diminished production of IFN-β in IRF-3-deficient mice might lead to increased viral damage to the heart in comparison to that observed in wild-type mice. To test this hypothesis, we examined reovirus-induced cardiac pathology in wild-type and IRF-3-deficient animals. Following p.o. inoculation of T1L, a mildly myocarditic strain, inflammatory lesions were visible on the hearts of IRF-3-deficient mice by day 12 postinoculation, whereas the hearts of wild-type mice appeared normal (Fig. 4A). Histologic sections of hearts resected from wild-type animals infected with T1L showed inflammatory lesions that distribute within regions of cells that stain for reovirus antigen and the activated form of caspase-3, consistent with mild myocarditis (Fig. 4B). In contrast, sections of the hearts from IRF-3-deficient mice displayed large lesions with almost complete tissue destruction and numerous cells that stain for reovirus and activated caspase-3. Regions that contained activated caspase-3 immunoreactivity also were positive by terminal deoxynucleotidyltransferase-mediated dUTP-biotin nick end labeling (TUNEL) assay (data not shown), which marks apoptotic DNA fragments, confirming that apoptosis is associated with these cardiac lesions. These findings suggest that IRF-3 attenuates reovirus-induced myocarditis.

Damage to the heart induced by reovirus infection of IRF-$3^{-/-}$ mice was independent of the route of inoculation. Following i.c. inoculation of mice with T1L, neither wild-type nor IRF-3-null animals displayed signs of CNS disease, and reovirus tropism in the CNS was not altered by the absence of IRF-3 (data not shown). In contrast, gross pathological lesions were observed in the hearts of i.c.-inoculated IRF-3-null mice (data not shown), suggesting that these animals succumbed to reovirus myocarditis.

Inhibition of reovirus-induced cardiac pathology in wild-type animals could be caused by a systemic IFN response induced at the initial site of replication or a localized response within cardiac tissue. To distinguish between these possibilities, we assayed IFN-β in the serum of reovirus-infected wild-type and IRF-3-null animals by ELISA. In these experiments, IFN-β was not detected in the serum of either mouse strain (data not shown). Therefore, we examined the induction of IFN-β and the IRF-3- and IFN-inducible gene, ISG56 (11), in cultures of primary myocytes derived from wild-type and IRF-3-deficient mice. Cultured myocytes were either mock infected or inoculated with T1L at an MOI of 10 PFU/cell, and RNA was extracted from the cultures at 8 and 24 h postinoculation. Both IFN-β and ISG56 were induced following infection of wild-type myocytes, whereas neither gene was induced in IRF-3-deficient myocytes (Fig. 5). These observations suggest that the observed differences in reovirus-induced myocarditis are in part attributable to decreased expression of IFN-β in myocytes.

In addition to their role in innate antiviral immunity, type I IFNs can prime the adaptive immune response (6, 18, 20). Therefore, the delay in clearance of reovirus in IRF-3-deficient mice might be due to dysregulated adaptive immune responses. To assess the functional capacity of the cell-mediated adaptive immune response elicited by reovirus in the presence and absence of IRF-3, we quantified IFN-γ-producing $CD8^+$ T cells following antigenic stimulation. On day 8 postinoculation, spleens were resected from mock- and T1L-infected wild-type and IRF-3-deficient animals, and splenocytes were isolated. Splenocytes were incubated with mock- or T1L-infected haplotype-matched fibroblasts in the presence of IL-2 and a protein secretion inhibitor. Splenocytes were fixed and stained using fluorescently conjugated anti-CD8 and IFN-γ antibodies and analyzed by flow cytometry (Fig. 6A). No significant differences were observed in the number of activated $CD8^+$ T cells in spleens from wild-type and IRF-3-deficient mice, indicating that the capacity of $CD8^+$ T cells to mount a cytokine response to antigen was not altered by the lack of IRF-3.

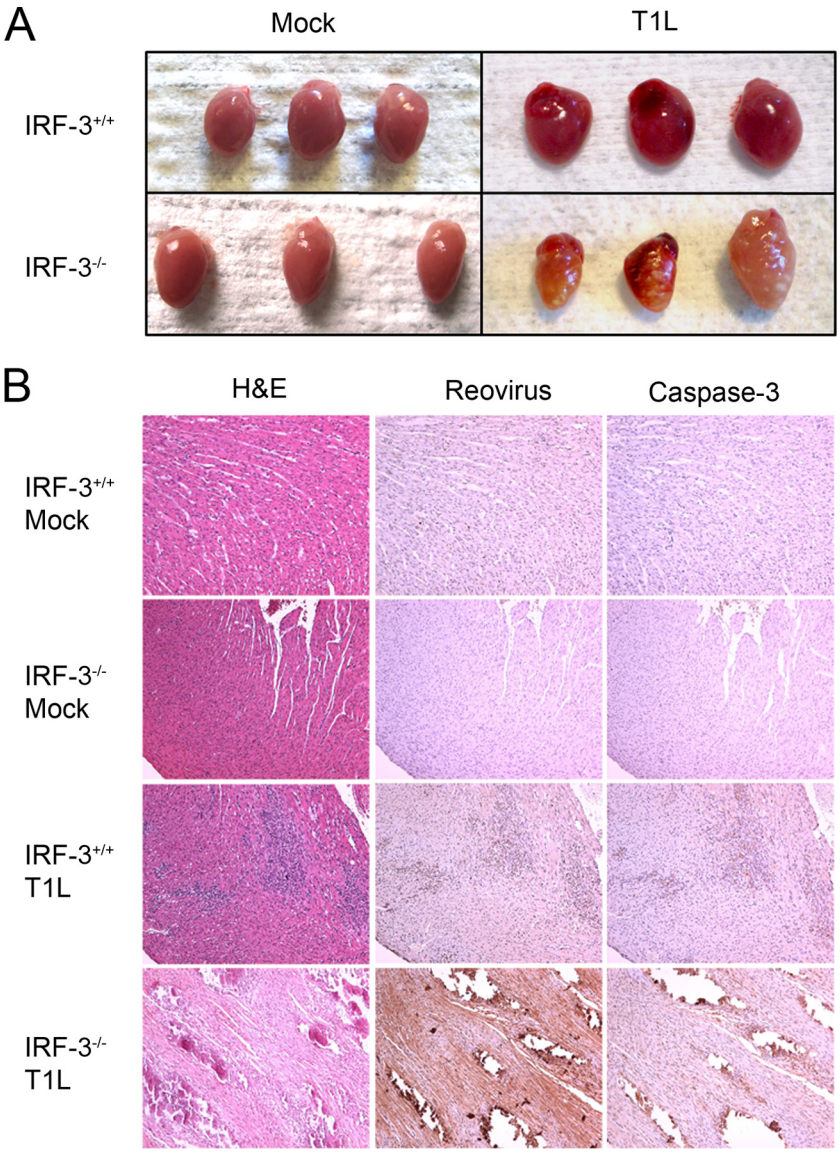

FIG. 4. IRF-3 attenuates reovirus myocarditis. Two-day-old IRF-$3^{+/+}$ and IRF-$3^{-/-}$ mice were inoculated p.o. with 10^7 PFU of T1L. On day 12 postinoculation, mice were euthanized, and hearts were resected and either photographed (A) or fixed in formalin, embedded in paraffin, sectioned, and stained with H&E, polyclonal reovirus-specific antiserum, or activated caspase-3-specific antibody (B).

To determine whether the humoral immune response was affected by the absence of IRF-3, we quantified reovirus-specific serum IgG titers in wild-type and IRF-3-deficient mice at days 8 and 12 postinoculation using a whole-virus ELISA (Fig. 6B). Serum IgG levels in wild-type and IRF-3-deficent mice did not differ at either of these time points. Collectively, these data suggest that neither $CD8^+$ T-cell nor B-cell functions are altered in IRF-3-deficient mice and suggest that a cell-intrinsic factor under IRF-3 control is required for efficient clearance of reovirus infection.

DISCUSSION

In this study, we found that innate immune response transcription factor IRF-3 attenuates disease caused by a mildly pathogenic reovirus strain, T1L, but not a highly pathogenic strain, T3SA+. Remarkably, T1L produces fulminant myocarditis in IRF-3-deficient mice regardless of the inoculation route (Fig. 4 and data not shown), indicating that IRF-3 exerts a key protective effect in the heart. IRF-3 also serves a critical function in reovirus clearance, which appears to be independent of IRF-3 effects on the development of an adaptive immune response. These findings point to a cell-intrinsic role for IRF-3 in the resolution of acute viral infection.

Innate immune responses serve a critical function in host defense against reovirus. Type I IFN protects mice from fatal reovirus challenge (15) and limits reovirus myocarditis (24, 32). In both primary murine fibroblasts and cardiac myocytes, IRF-3 is required for IFN-β expression in response to reovirus (13, 23). Our data demonstrate that IRF-3 is required for maximal induction of IFN-β mRNA in the intestine following reovirus infection, which correlates with lower viral titers at

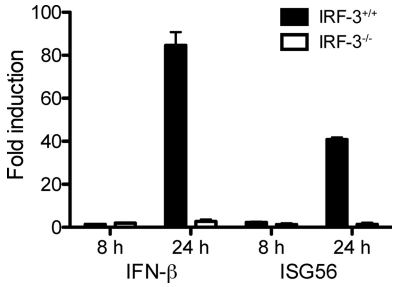

FIG. 5. IRF-3 is required for IFN-β and ISG expression in primary cardiac myocytes. Duplicate wells of primary cardiac myocyte cultures were either mock infected or inoculated with T1L at an MOI of 10 PFU/cell. At the indicated times postinoculation, total RNA was harvested for qRT-PCR. The C_Ts for IFN-β and ISG56 were normalized to those for GAPDH for each sample. Reovirus-infected samples were compared to mock-infected samples harvested at the same time postinoculation to calculate fold induction. Results are expressed as the mean fold induction for duplicate wells. Error bars indicate the standard deviation (SD). Results are representative of duplicate experiments.

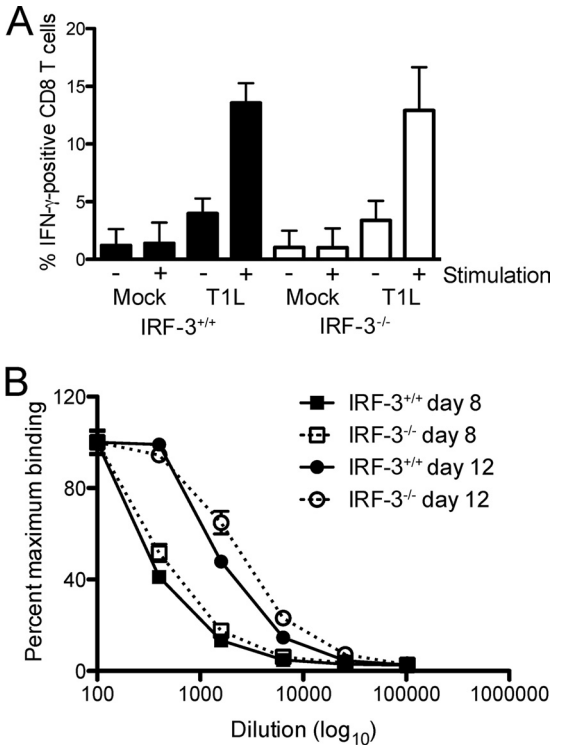

FIG. 6. IRF-3 deficiency does not alter the functional capacity of the adaptive immune response to reovirus. Two-day-old IRF-$3^{+/+}$ and IRF-$3^{-/-}$ mice were inoculated p.o. with PBS or 10^7 PFU of T1L. (A) On day 8 postinoculation, mice were euthanized, spleens were resected, and splenocytes were isolated. Splenocytes were incubated with mock-infected or T1L-infected fibroblasts for 5 h and stained with CD8-PE and anti-IFN-γ–FITC. Results are expressed as the mean percentage of IFN-γ-positive $CD8^+$ T cells from three independent experiments of five mice each. Error bars indicate SD. (B) On days 8 and 12 postinoculation, mice were euthanized, and blood samples were collected. IgG titer in sera was determined by whole-virus ELISA. Results are expressed as the mean percentage of the maximal optical density (OD) for 4-fold dilutions, starting at 1:100, for six to seven mice. Error bars indicate the standard error of the mean (SEM).

that site. However, mice lacking IRF-3 are capable of expressing some IFN-β mRNA, albeit at levels significantly lower than those expressed by wild-type mice. It is possible that other mechanisms, such as constitutive expression of IRF-7 in some cell types, may compensate for the lack of IRF-3 in these animals. These findings are consistent with studies of other RNA viruses in which near wild-type levels of IFN-β are observed following infection of IRF-3-deficient mice (7, 14).

Clearance of reovirus from the intestine is mediated by components of both cell-mediated and humoral immunity (2, 10, 14). In newborn mice, monoclonal IgG antibodies can protect against reovirus disease, even if administered following inoculation of the virus (30, 34). However, adoptive transfer of immune splenocytes limits reovirus replication in the neonatal intestine even more efficiently than treatment with monoclonal antibodies (37). Slightly different results were gathered in infection studies using adult SCID mice. In this model, $CD8^+$ T-cell deficiency has no effect on intestinal clearance of reovirus (2), and neither NK cells nor macrophages can prevent lethal infection (10). Instead, B cells and systemic IgG appear to mediate intestinal clearance (2). In addition to cell-mediated and humoral immunity, innate immune mechanisms also contribute to clearance of reovirus. IFN produced by Peyer's patch conventional and plasmacytoid dendritic cells is required for efficient reovirus clearance and control of intestinal infection (15). Together with results presented here, these data suggest that the adaptive immune response is not sufficient to effect viral clearance and that innate immune processes are required for both the initiation of the immune response and resolution of infection.

Innate immune processes can dictate organ- and cell-type-specific differences in reovirus disease. Cell culture models of reovirus infection have ascribed proapoptotic functions to both NF-κB and IRF-3 in a variety of cell types, including both immortalized cell lines and primary murine embryonic fibroblasts (5, 12, 13). NF-κB also mediates a proapoptotic response to reovirus infection in the CNS of neonatal mice (24). We did not observe differences in CNS pathology in wild-type and IRF-3-deficient mice, likely because T1L is not neurotropic and does not induce apoptosis in the CNS. However, in the myocardium, NF-κB protects against apoptotic injury (24), and our results suggest that IRF-3 has a similar function.

There are three possible mechanisms that might account for the discrepancy between the requirement for NF-κB and IRF-3 in apoptosis induction in cell culture versus the neonatal heart. First, virus-induced activation of cell-intrinsic apoptotic processes might differ in cardiac myocytes and other cell types. In myocytes, activation of NF-κB and IRF-3 may skew the cellular response toward initiating and maintaining an antiviral state rather than promoting apoptosis. This antiviral function may spare cardiac myocytes, a nonregenerating cell population, from viral injury as a means of maintaining cardiac function. In the absence of these antiviral pathways, virus replication is prolonged, as suggested by the increased virus titers in the heart at late times postinfection. Prolonged infection also may alter other cellular metabolic or signaling pathways capable of initiating programmed cell death.

Second, apoptosis observed in myocardial lesions may result from extrinsic cell-death pathways induced by inflammatory

mediators, such as tumor necrosis factor, or cell-mediated killing. Although reovirus myocarditis is usually associated with only modest inflammatory infiltrates (24, 30) and does not require adaptive immune components (30), the absence of IRF-3-dependent gene expression may exacerbate these mechanisms. These inflammatory processes, which are not relevant in cell culture, also may be accentuated by the prolonged presence of reovirus antigen, similar to the coxsackievirus B model of persistent myocardial injury (17).

Third, and finally, IRF-3 might induce an early proapoptotic response to reovirus infection in cardiac cells, which functions to enhance immune-mediated clearance of infected cells. This apoptotic response may be at the threshold of detection by immunohistochemical staining, as few caspase-3- or TUNEL-positive cells were observed in heart sections of wild-type mice during early stages of infection, perhaps because apoptotic cells are rapidly cleared to prevent virus spread. In this scenario, the lack of an early proapoptotic IRF-3 response would prolong viral replication in the heart and lead to the observed defect in virus clearance at late times postinfection. Importantly, in each of these possibilities, the IRF-3/IFN-β response is essential for controlling levels of virus replication and myocardial damage.

Within the heart, cell types such as myocytes and fibroblasts respond differently to reovirus infection, based on basal expression levels of components of the IFN signaling circuit (43) and additional undefined differences (22). Cell-type-dependent basal expression of ISGs, such as ISG56, and pattern recognition proteins, such as RIG-I, is controlled by IRF-3 (7). Our results indicate that induction of both IFN-β and ISG56 is reduced in IRF-3-null cardiac myocytes. These data suggest that the IFN response limits T1L-mediated disease. Moreover, T1L induces much lower levels of IFN-β mRNA than does prototype type 3 strain type 3 Dearing in wild-type myocytes, as measured by qRT-PCR (data not shown). Although this experiment does not address whether differences in IFN-β induction result from differences in the total number of cells producing IFN or levels of IFN produced by individual cells, these findings suggest that even minimal IFN induction can lead to protection. Since adaptive immune responses to reovirus appear unaffected by the absence of IRF-3, it is likely that these cell-intrinsic functions of IRF-3 are required for efficient reovirus clearance.

Differences in cell-intrinsic innate immune responses also appear to influence the relative pathogenicity of reovirus serotypes. Reovirus strain T1L is mildly pathogenic following p.o. inoculation in the presence of an intact innate immune system, but the absence of IRF-3 renders this virus capable of causing a lethal infection. In contrast, while IRF-3 deficiency exacerbates infection with the highly pathogenic strain T3SA+, leading to increased titers in several organs (data not shown), activation of IRF-3 is not sufficient to overcome the increased pathogenicity of this strain. It is possible that differences in cell tropism exhibited by T1L and T3SA+ account for the differential effects of IRF-3. In the murine CNS, T1L infects ependymal cells lining the cerebral ventricles, whereas T3SA+ infects neurons and causes lethal encephalitis (3, 41, 42). IRF-3 expression may restrict T1L infection of its cellular targets, whereas it may not be sufficient to limit T3SA+ infection at the sites it infects. This effect is likely IFN independent, because in some cell types, including cardiac myocytes, T1L has a greater replication capacity and is less sensitive to the antiviral effects of IFN than are type 3 strains. Additionally, T1L antagonizes the IFN signaling response (44), suggesting that IRF-3 impedes T1L replication independently of IFN. Alternatively, IRF-3 deficiency may alter the capacity of T1L to induce apoptosis. T1L is a weak inducer of apoptosis in cell culture (35) and does not induce apoptosis in primary rat cardiac myocytes (4). However, myocardial lesions caused by T1L in IRF-3-null mice contain activated caspase-3 and are TUNEL positive (Fig. 4 and data not shown), suggesting that T1L-mediated pathogenicity is caused by a greater capacity to induce apoptotic injury in the absence of IRF-3.

Results presented here suggest that IRF-3 mediates the initiation of antiviral responses early in infection and facilitates clearance of reovirus. The latter effect appears to be independent of the development of antiviral $CD8^+$ T-cell responses and serum IgG. Together with previous reports, these data suggest that cell-intrinsic effects of IRF-3 are essential for containment of viral infection.

ACKNOWLEDGMENTS

We thank members of our laboratories for many helpful discussions and Dean Ballard, Wrennie Edwards, Lance Johnson, Yanice Mendez-Fernandez, Claudio Mosse, and Luc Van Kaer for technical assistance, reagents, and advice.

This research was supported by Public Health Service awards T32 AI49824 (G.H.H.), F32 AI071440 (G.H.H.), R01 AI62657 (B.S.), and R01 AI50080 (T.S.D.) and the Elizabeth B. Lamb Center for Pediatric Research. Additional support was provided by Public Health Service award P30 CA68485 for the Vanderbilt-Ingram Cancer Center and P60 DK20593 for the Vanderbilt Diabetes Research and Training Center.

We have no financial conflicts of interest.

REFERENCES

1. **Antar, A. A. R., J. L. Konopka, J. A. Campbell, R. A. Henry, A. L. Perdigoto, B. D. Carter, A. Pozzi, T. W. Abel, and T. S. Dermody.** 2009. Junctional adhesion molecule-A is required for hematogenous dissemination of reovirus. Cell Host Microbe **5:**59–71.
2. **Barkon, M., B. Haller, and H. Virgin IV.** 1996. Circulating immunoglobulin G can play a critical role in clearance of intestinal reovirus infection. J. Virol. **70:**1109–1116.
3. **Barton, E. S., B. E. Youree, D. H. Ebert, J. C. Forrest, J. L. Connolly, T. Valyi-Nagy, K. Washington, J. D. Wetzel, and T. S. Dermody.** 2003. Utilization of sialic acid as a coreceptor is required for reovirus-induced biliary disease. J. Clin. Invest. **111:**1823–1833.
4. **Clarke, P., R. L. Debiasi, S. M. Meintzer, B. A. Robinson, and K. L. Tyler.** 2005. Inhibition of NF-kappa B activity and cFLIP expression contribute to viral-induced apoptosis. Apoptosis **10:**513–524.
5. **Connolly, J. L., S. E. Rodgers, P. Clarke, D. W. Ballard, L. D. Kerr, K. L. Tyler, and T. S. Dermody.** 2000. Reovirus-induced apoptosis requires activation of transcription factor NF-kB. J. Virol. **74:**2981–2989.
6. **Curtsinger, J. M., J. O. Valenzuela, P. Agarwal, D. Lins, and M. F. Mescher.** 2005. Cutting edge: type I IFNs provide a third signal to CD8 T cells to stimulate clonal expansion and differentiation. J. Immunol. **174:**4465–4469.
7. **Daffis, S., M. A. Samuel, B. C. Keller, M. Gale, Jr., and M. S. Diamond.** 2007. Cell-specific IRF-3 responses protect against West Nile virus infection by interferon-dependent and -independent mechanisms. PLoS Pathog. **3:**e106.
8. **Danthi, P., C. M. Coffey, J. S. L. Parker, T. W. Abel, and T. S. Dermody.** 2008. Independent regulation of reovirus membrane penetration and apoptosis by the μ1 φ domain. PLoS Pathog. **4:**e1000248.
9. **Edelmann, K. H., S. Richardson-Burns, L. Alexopoulou, K. L. Tyler, R. A. Flavell, and M. B. Oldstone.** 2004. Does Toll-like receptor 3 play a biological role in virus infections? Virology **322:**231–238.
10. **George, A., S. I. Kost, C. L. Witzleben, J. J. Cebra, and D. H. Rubin.** 1990. Reovirus-induced liver disease in severe combined immunodeficient (SCID) mice. A model for the study of viral infection, pathogenesis, and clearance. J. Exp. Med. **171:**929–934.
11. **Grandvaux, N., M. J. Servant, B. tenOever, G. C. Sen, S. Balachandran, G. N. Barber, R. Lin, and J. Hiscott.** 2002. Transcriptional profiling of

interferon regulatory factor 3 target genes: direct involvement in the regulation of interferon-stimulated genes. J. Virol. **76:**5532–5539.
12. **Hansberger, M. W., J. A. Campbell, P. Danthi, P. Arrate, K. N. Pennington, K. B. Marcu, D. W. Ballard, and T. S. Dermody.** 2007. IκB kinase subunits α and γ are required for activation of NF-κB and induction of apoptosis by mammalian reovirus. J. Virol. **81:**1360–1371.
13. **Holm, G. H., J. Zurney, V. Tumilasci, P. Danthi, J. Hiscott, B. Sherry, and T. S. Dermody.** 2007. Retinoic acid-inducible gene-I and interferon-b promoter stimulator-1 augment proapoptotic responses following mammalian reovirus infection via interferon regulatory factor-3. J. Biol. Chem. **282:** 21953–21961.
14. **Honda, K., H. Yanai, H. Negishi, M. Asagiri, M. Sato, T. Mizutani, N. Shimada, Y. Ohba, A. Takaoka, N. Yoshida, and T. Taniguchi.** 2005. IRF-7 is the master regulator of type-I interferon-dependent immune responses. Nature **434:**772–777.
15. **Johansson, C., J. D. Wetzel, C. Mikacenic, J. P. He, T. S. Dermody, and B. Kelsall.** 2007. Type I interferons produced by hematopoietic cells protect mice against lethal infection by mammalian reovirus. J. Exp. Med. **204:**1349–1358.
16. **Kilham, L., and G. Margolis.** 1969. Hydrocephalus in hamsters, ferrets, rats, and mice following inoculations with reovirus type 1. Lab. Invest. **22:**183–188.
17. **Klingel, K., C. Hohenadl, A. Canu, M. Albrecht, M. Seemann, G. Mall, and R. Kandolf.** 1992. Ongoing enterovirus-induced myocarditis is associated with persistent heart muscle infection: quantitative analysis of virus replication, tissue damage, and inflammation. Proc. Natl. Acad. Sci. U. S. A. **89:**314–318.
18. **Le Bon, A., N. Etchart, C. Rossmann, M. Ashton, S. Hou, D. Gewert, P. Borrow, and D. F. Tough.** 2003. Cross-priming of $CD8^+$ T cells stimulated by virus-induced type I interferon. Nat. Immunol. **4:**1009–1015.
19. **Loo, Y. M., J. Fornek, N. Crochet, G. Bajwa, O. Perwitasari, L. Martinez-Sobrido, S. Akira, M. A. Gill, A. Garcia-Sastre, M. G. Katze, and M. Gale, Jr.** 2008. Distinct RIG-I and MDA5 signaling by RNA viruses in innate immunity. J. Virol. **82:**335–345.
20. **Luft, T., K. C. Pang, E. Thomas, P. Hertzog, D. N. J. Hart, J. Trapani, and J. Cebon.** 1998. Type I IFNs enhance the terminal differentiation of dendritic cells. J. Immunol. **161:**1947–1953.
21. **Marié, I., J. E. Durbin, and D. E. Levy.** 1998. Differential viral induction of distinct interferon-alpha genes by positive feedback through interferon regulatory factor-7. EMBO J. **17:**6660–6669.
22. **Miyamoto, S. D., R. D. Brown, B. A. Robinson, K. L. Tyler, C. S. Long, and R. L. Debiasi.** 2009. Cardiac cell-specific apoptotic and cytokine responses to reovirus infection: determinants of myocarditic phenotype. J. Card. Fail. **15:**529–539.
23. **Noah, D. L., M. A. Blum, and B. Sherry.** 1999. Interferon regulatory factor 3 is required for viral induction of beta interferon in primary cardiac myocyte cultures. J. Virol. **73:**10208–10213.
24. **O'Donnell, S. M., M. W. Hansberger, J. L. Connolly, J. D. Chappell, M. J. Watson, J. M. Pierce, J. D. Wetzel, W. Han, E. S. Barton, J. C. Forrest, T. Valyi-Nagy, F. E. Yull, T. S. Blackwell, J. N. Rottman, B. Sherry, and T. S. Dermody.** 2005. Organ-specific roles for transcription factor NF-κB in reovirus-induced apoptosis and disease. J. Clin. Invest. **115:**2341–2350.
25. **O'Donnell, S. M., G. H. Holm, J. M. Pierce, B. Tian, M. J. Watson, R. S. Chari, D. W. Ballard, A. R. Brasier, and T. S. Dermody.** 2006. Identification of an NF-κB-dependent gene network in cells infected by mammalian reovirus. J. Virol. **80:**1077–1086.
26. **Rubin, D. H., and B. N. Fields.** 1980. Molecular basis of reovirus virulence: role of the M2 gene. J. Exp. Med. **152:**853–868.
27. **Sato, M., H. Suemori, N. Hata, M. Asagiri, K. Ogasawara, K. Nakao, T. Nakaya, M. Katsuki, S. Noguchi, N. Tanaka, and T. Taniguchi.** 2000. Distinct and essential roles of transcription factors IRF-3 and IRF-7 in response to viruses for IFN-alpha/beta gene induction. Immunity **13:**539–548.
28. **Sato, M., N. Tanaka, N. Hata, E. Oda, and T. Taniguchi.** 1998. Involvement of the IRF family transcription factor IRF-3 in virus-induced activation of the IFN-β gene. FEBS Lett. **425:**112–116.
29. **Schiff, L. A., M. L. Nibert, and K. L. Tyler.** 2007. Orthoreoviruses and their replication, p. 1852–1915. *In* D. M. Knipe and P. M. Howley (ed.), Fields virology, 5th ed., vol. 2. Lippincott, Williams, and Wilkins, Philadelphia, PA.
30. **Sherry, B., X. Y. Li, K. L. Tyler, J. M. Cullen, and H. W. Virgin.** 1993. Lymphocytes protect against and are not required for reovirus-induced myocarditis. J. Virol. **67:**6119–6124.
31. **Sherry, B., F. J. Schoen, E. Wenske, and B. N. Fields.** 1989. Derivation and characterization of an efficiently myocarditic reovirus variant. J. Virol. **63:** 4840–4849.
32. **Sherry, B., J. Torres, and M. A. Blum.** 1998. Reovirus induction of and sensitivity to beta interferon in cardiac myocyte cultures correlate with induction of myocarditis and are determined by viral core proteins. J. Virol. **72:**1314–1323.
33. **Tyler, K. L., R. T. Bronson, K. B. Byers, and B. N. Fields.** 1985. Molecular basis of viral neurotropism: experimental reovirus infection. Neurology **35:** 88–92.
34. **Tyler, K. L., M. A. Mann, B. N. Fields, and H. W. Virgin, I. V.** 1993. Protective anti-reovirus monoclonal antbodies and their effects on viral pathogenesis. J. Virol. **67:**3446–3453.
35. **Tyler, K. L., M. K. Squier, S. E. Rodgers, S. E. Schneider, S. M. Oberhaus, T. A. Grdina, J. J. Cohen, and T. S. Dermody.** 1995. Differences in the capacity of reovirus strains to induce apoptosis are determined by the viral attachment protein s1. J. Virol. **69:**6972–6979.
36. **Virgin, H. W., IV, R. Bassel-Duby, B. N. Fields, and K. L. Tyler.** 1988. Antibody protects against lethal infection with the neurally spreading reovirus type 3 (Dearing). J. Virol. **62:**4594–4604.
37. **Virgin, H. W., IV, M. A. Mann, B. N. Fields, and K. L. Tyler.** 1991. Monoclonal antibodies to reovirus reveal structure/function relationships between capsid proteins and genetics of susceptibility to antibody action. J. Virol. **65:**6772–6781.
38. **Virgin, H. W., T. S. Dermody, and K. L. Tyler.** 1998. Cellular and humoral immunity to reovirus infection. Curr. Top. Microbiol. Immunol. **233:**147–161.
39. **Virgin, H. W., and K. L. Tyler.** 1991. Role of immune cells in protection against and control of reovirus infection in neonatal mice. J. Virol. **65:**5157–5164.
40. **Virgin, H. W., K. L. Tyler, and T. S. Dermody.** 1997. Reovirus, p. 669–699. *In* N. Nathanson (ed.), Viral pathogenesis. Lippincott-Raven, New York, NY.
41. **Weiner, H. L., D. Drayna, D. R. Averill, Jr., and B. N. Fields.** 1977. Molecular basis of reovirus virulence: role of the S1 gene. Proc. Natl. Acad. Sci. U. S. A. **74:**5744–5748.
42. **Weiner, H. L., M. L. Powers, and B. N. Fields.** 1980. Absolute linkage of virulence and central nervous system tropism of reoviruses to viral hemagglutinin. J. Infect. Dis. **141:**609–616.
43. **Zurney, J., K. E. Howard, and B. Sherry.** 2007. Basal expression levels of IFNAR and Jak-STAT components are determinants of cell-type-specific differences in cardiac antiviral responses. J. Virol. **81:**13668–13680.
44. **Zurney, J., T. Kobayashi, G. H. Holm, T. S. Dermody, and B. Sherry.** 2009. The reovirus μ2 protein inhibits interferon signaling through a novel mechanism involving nuclear accumulation of interferon regulatory factor 9. J. Virol. **83:**2178–2187.